Heat Transfer Engineering, 00(00):1–10, 2016

ISSN: 0145-7632 print / 1521-0537 online
DOI: 10.1080/01457632.2015.1066650

Taylor & Francis
Taylor & Francis Group

Cycle Optimization on Reheat Adsorption Cycle Applying Fixed Chilled Water Outlet Temperature

I GUSTI AGUNG BAGUS WIRAJATI,[1,3] YUKI UEDA,[1] ATSUSHI AKISAWA,[1] and TAKAHIKO MIYAZAKI[2]

[1]Graduate School of Bio-Applications and Systems Engineering, Tokyo University of Agriculture and Technology, Tokyo, Japan
[2]Department of Energy and Material Sciences, Kyushu University, Fukuoka, Japan
[3]Bali State Polytechnic, Bali, Indonesia

This study investigated the cycle optimization of four-bed, silica gel–water adsorption with reheat cycle, where the desorber (upper bed) and adsorber (lower bed) always interact with the condenser and evaporator, to exploit a low heat-source temperature. In a previous study, the performance of a reheat cycle with chilled water outlet temperature fixed at 9°C was observed without considering the cycle optimization. Maintaining a constant chilled water outlet temperature is also of equal importance to improve the conversion efficiency so that maximum cooling capacity can be derived. In this paper, a simulation model of reheat adsorption cycles is developed to analyze the optimization of the cycle time, including adsorption/desorption time, mass recovery time, and preheating/precooling time, with chilled water outlet temperature fixed. The reheat working principle is also introduced. The proposed cycle is compared with the four-bed versison without reheat cycle in terms of coefficient of performance (COP) and cooling capacity. The result shows that the performance of a reheat cycle is superior to that of four-bed version without reheat, especially for low heat-source temperature. For low heat-source temperature (55–65°C) both COP and cooling capacity of the reheat cycle with optimization were raised significantly compared to the high heat-source temperature (70–80°C).

INTRODUCTION

The use of an adsorption chiller, well known as an environmentally friendly chiller, has become popular in past decades because of its features such as low heat-source temperature utilized, super energy saving, using neither cholorfluorocarbons (CFCs) nor hydrochlorofluorocarbons (HCFCs), easy maintenance, and safety [1, 2]. The adsorption refrigeration chiller system is regarded not only as an alternative for reducing CFCs and HCFCs uses but also as an energy-efficient technology [3]. Furthermore, an adsorption cycle has a distinct advantage over other systems for its ability to be driven by heat of relatively low, near-environmental temperatures, which can be recovered, which is highly desirable and investigated by Kashiwagi et al. [4].

There are some popular adsorbate–refrigerant pairs for air conditioning and refrigeration purposes, such as silica gel–water, zeolite–water, activated carbon–ammonia, and so on. For utilizing a heat-source temperature below 100°C, only silica gel–water is the closest, useful and very suitable as the adsorbate–refrigerant pair compared to the other pairs [5–9]. Therefore, silica gel–water is chosen because the regeneration temperature of silica gel is lower than that of activated carbon, and water has large latent heat of vaporization.

The performance characteristics and the cycle operating conditions of the adsorption chiller have investigated by Saha et al. [10, 11]. It was shown that the cycle time is one of the most influential parameters on the performance of the adsorption chiller. The performance model considering the operating condition effects has observed by Ahmed and Raya [12], who concluded that the optimum cycle time of a two-bed

Address correspondence to Professor Atsushi Akisawa, Graduate School of Bio-Applications and Systems Engineering, Tokyo University of Agriculture and Technology, 2-24-16 Naka-cho, Koganei-shi 184-8588, Tokyo, Japan. E-mail: akisawa@cc.tuat.ac.jp

adsorption chiller corresponding to maximum cooling capacity was increased significantly. Meanwhile, Rahman et al. [13] introduced the performance comparison of an adsorption cooling system with optimization and concluded that time allocation of the cycle is relatively sensitive to the variation of heat-source temperature.

The preheating/precooling time also affected the performance of the adsorption chiller, as investigated by Alam et al. [14]. The performance of an advanced adsorption chiller, namely, the reheat cycle, has been investigated by Alam et al. [15], Uyun et al. [16], and Khan et al. [17]. However, optimization of the cycle was never done and chilled water outlet temperatures as arranged fluctuated. Maintaining a constant chilled water outlet temperature is also of equal importance to improve the conversion efficiency so that maximum cooling capacity can be derived [18]. Wirajati et al. [19] identified the effect of the heat-source temperature and the effect of cycle time on performance if the chilled water outlet temperature is fixed at 9°C experimentally and showed that the performance of the chiller improved with increasing heat-source temperature and that a total cycle time between 2000 to 2500 s yields better performance for the chiller. Waste heat below 100°C is considered for the driving heat source due to effective cooling production.

The objectives of this study are (1) to develop a simulation numerically of a four-adsorber/desorber reheat adsorption cycle, (2) to optimize the cycle time, and (3) to compare the proposed optimized cycle with the optimized four-adsorber/desorber conventional cycle. The optimization of the four-bed reheat cycle is focusing on adsorption/desorption time, mass recovery time, and preheating/precooling time, especially in chilled water of temperature 9°C.

As a result, to gain chilled water of fixed temperature, controlling the mass flow rate is taken into account and cycle optimization of the reheat cycle has offered better performance in terms of both coefficient of performance (COP) and cooling capacity. A heat-source temperature of 55°C showed the highest increment of 80% rise in both COP and cooling capacity after being optimized. For low heat-source temperature, applying cycle time unification should be selected carefully.

WORKING PRINCIPLE AND OPERATIONAL STRATEGY OF THE REHEAT ADSORPTION CYCLE

Figure 1a shows the reheat adsorption cycle scheme. The chiller consists of four heat exchangers (i.e., HEX1, HEX2, HEX3, and HEX4), one condenser, and one evaporator. The adsorbent heat exchangers of the chiller are operated through six thermodynamic processes in a full cycle, namely, adsorption, mass recovery with cooling, preheating, desorption, mass recovery with heating, and precooling. In the adsorption process, the refrigerant (water) is evaporated in an evaporator at the temperature T_{eva} and seizes heat (Q_{eva}) from the chilled water isobarically. An evaporation process occurs and produces a cooling effect. Evaporation heat is supplied by flowing chilled water of low heat-source temperature. In first-half cycle, HEX1 is heated by hot water and HEX3 is cooled by cooling water. When the pressures of HEX1 and HEX3 are nearly equal, both are then connected by opening the connecting valve, allowing vapor flow from HEX1 into HEX3. This process is known as the mass recovery process.

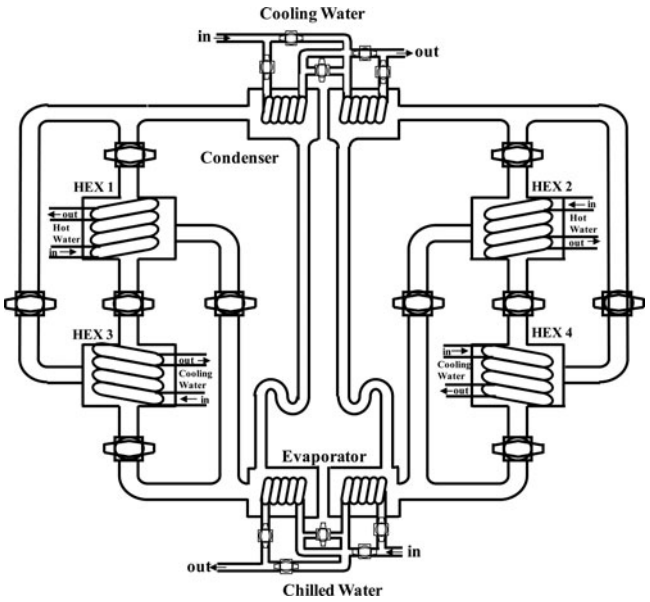

Figure 1 Reheat adsorption cycle scheme.

The heating and cooling process is continued during the mass recovery process. HEX1 is heated up by hot water and HEX3 is cooled down by cooling water to provide more cooling capacities. During this process, refrigerant circulation is stopped by closing all refrigerant valves. This process is known as the preheating/precooling process.

When the pressures of HEX1 and HEX3 are nearly equal to the pressures of condenser and evaporator, the valve between HEX1 and condenser (as well as the valve between HEX3 and evaporator) is opened, allowing refrigerant to flow. The adsorption and desorption process then starts. In this process, refrigerant from HEX1 will be transferred in the condenser and then it will be condensed by releasing heat to the heat sink. Finally, the liquid refrigerant flows from the condenser to evaporator through U-shaped tube to control pressure difference between condenser and evaporator. To complete a full cycle, the next process is the same as the first half-cycle by change the position of HEX3 as a desorber and HEX1 as an adsorber. HEX2 and HEX4 are also following the similar process of HEX 1 and HEX 3 in the full cycle.

Table 1 represents the operational strategy of reheat cycles, which consists of 10 modes (modes A–J).

In modes A and B, HEX1 and HEX3 are in the desorption and adsorption process while HEX2 and HEX4 are completing mass recovery heating/cooling and the precooling/preheating process. Mode C, after completing mass

Table 1 Operational strategy of reheat cycle

HEX	Mode									
	A	B	C	D	E	F	G	H	I	J
1	Des			Mrh	Pc	Ads			Mrc	Ph
2	Mrh	Pc		Ads		Mrc	Ph		Des	
3	Ads			Mrc	Ph	Des			Mrh	Pc
4	Mrc	Ph		Des		Mrh	Pc		Ads	

Note. Ads = adsorption; Mrh = mass recovery heating; Pc = precooling; Des = desorption; Mrc = mass recovery cooling; and Ph = preheating.

recovery and the preheating/precooling process for HEX2 and HEX4, is then continuing the adsorption and desorption process simultaneously with HEX1 and HEX3. Mode C and mode H are the special characteristics of the operational strategy of this cycle because there are two HEXs doing the adsorption and desorption process at the same time (mode C and mode H). In mode D and mode E, HEX2 and HEX4 are doing the adsorption and desorption process while HEX1 and HEX3 are doing mass recovery heating/cooling and the precooling/preheating process. Mode E is the first half cycle. In the second half cycle (i.e., mode F to J), HEX pair 1 and 3 acts the same as HEX pair 2 and 4 and vice versa.

Table 2 and Table 3 constitute the baseline parameter and standard operating conditions adapted in the simulation, respectively.

Table 2 Parameter values in simulation

Symbol	Value	Unit
C_s	924	J/kg-K
C_v	1.89E+03	J/kg-K
C_w	4.18E+03	J/kg-K
D_o	2.54E-4	m^2/s
E_a	4.20E+04	J/mol
L_w	2.50E+06	J/kg
Q_s	2.86E+06	J/kg
R	8.314	J/mol-K
R_p	3.00E-04	m
UA_{ads}	2001	W/K^2
UA_{des}	2233	W/K^2
UA_{eva}	2360.75	W/K^2
UA_{con}	4061.86	W/K^2
W_s	16	kg
$W_{con,w}$	5	kg
$W_{eva,w}$	25	kg

Table 3 Standard operating conditions

	Temperature (°C)	Flow rate (kg/s)
Hot water	60	1
Cooling water	30	1(ads) + 0.8(des)
Chilled water	14	0.8
Cycle time (Ads/Des + Mrc/Mrh + Ph/Pc)	(420 + 200 + 30) s	

Note. Ads/Des = adsorption/desorption. Mrc/Mrh = mass recovery. Ph/Pc = preheating/precooling.

SIMULATION EQUATION

Adsorber/Desorber Energy Balance

The heat transfer equation of adsorbent bed can be described as follows:

$$T_o = T + (T_i - T)\ \exp\left(\frac{U_{bed}A_{bed}}{\dot{m}_w.C_w}\right) \tag{1}$$

Here, T denotes bed temperature. The adsorbent bed temperature, pressure, and concentration are assumed to be uniform throughout the adsorbent bed. We have taken the specific heat of refrigerant (water) in the liquid phase as our system works in the low concentration range. Heat transfer fluid (water) temperature term T_i and T_o denote cooling water upon adsorption and hot water upon desorption.

The energy balance equation of adsorbent bed is shown here:

$$\left(W_s.C_s + W_w.C_w.q + W_{bed}.C_{bed}\right)\frac{dT}{dt}$$

$$= W_s.Q_s\frac{dq}{dT} - W_w.C_v.\delta\left[\gamma\left(T - T_{eva}\right)\left(T - T_{wv}\right)\right]\frac{dq}{dT}$$

$$+\dot{m}_w.C_w.\varepsilon_{bed}\left(T_i - T\right) \tag{2}$$

where δ is either 0 or 1 depending whether the adsorbent bed is working as a desorber or adsorber and γ is either 1 or 0 depending on whether the bed is connected with the evaporator or another bed. Equation (1) expresses the importance of heat transfer parameters, namely, heat transfer area A_{bed} and overall heat transfer coefficient U_{bed}. The left-hand side of the adsorber/desorber energy balance equations (Eq. (2)) provides the amount of sensible heat required to cool or heat the silica gel (s), water (w), and metallic (bed) parts of the heat exchanger during adsorption or desorption. This term accounts for the input/output of sensible heat required by the batched-cycle operation. The first term on the right-hand side of Eq. (2) constitutes the release of adsorption heat or the input of desorption heat, while the second terms accounts for the sensible heat of the adsorbed vapor. The last term on the right-hand side of Eq. (2) refers to the total amount of heat released into the cooling water upon adsorption or provided by the hot water for desorption. Equation (2) does not account for external heat losses into the environment, as

all the beds are considered to be well insulated; ε_{bed} in Eq. (2) expresses the heat exchanger effectiveness that came from the log mean temperature difference of heat exchanger (bed) in the flow system.

Condenser Energy Balance

Equation (3) represents as the heat transfer of the condenser while Eq. (4) shows energy balances for the condenser, and can be expressed as

$$T_{con,o} = T_{con} + \left(T_{cw,i} - T_{con}\right) \exp\left(\frac{U_{con}A_{con}}{\dot{m}_w.c_w}\right) \tag{3}$$

$$\left(W_{con,w}.C_w + W_{con,bed}.C_{con,bed}\right)\frac{dT_c}{dt} = \dot{m}_{cw}.C_w\,\varepsilon_{con} \times \left(T_{cw,i} - T_{cw,o}\right) - LW_s\frac{dq_{des}}{dT} - W_sC_v\left(T_{des} - T_{con}\right)\frac{dq_{des}}{dT} \tag{4}$$

The first term on the right-hand side of Eq. (4) gives the amount of heat released into the cooling water, the second term accounts for the latent heat of vaporization (L) for the amount of refrigerants desorbed (dq_{des}/dT) and the amount of heat that the liquid condensates carries away when it leaves the condenser to the evaporator. The term ε_{con} in Eq. (4) expresses the heat exchanger effectiveness that came from the log mean temperature difference of heat exchanger (condenser) in the flow system. The left-hand side of Eq. (4) represents the sensible heat required by the metallic parts of heat exchanger tubes due to the temperature variations in the condenser.

Evaporator Energy Balance

Equation (5) represents the heat transfer of the evaporator and Eq. (6) the energy balances for the evaporator, respectively:

$$T_{chill,o} = T_{eva} + \left(T_{chill,i} - T_{eva}\right) \exp\left(\frac{U_{eva}A_{eva}}{\dot{m}_{ch}.C_{ch}}\right) \tag{5}$$

$$\left(W_{eva,w}.C_w + W_{eva,bed}.C_{eva,bed}\right)\frac{dT_e}{dt} = \dot{m}_{chill}.C_{chill}.\varepsilon_{eva}\left(T_{chill,i} - T_{chill,o}\right) - LW_s\frac{dq_{ads}}{dT} - W_sC_v\left(T_{des} - T_{con}\right)\frac{dq_{des}}{dT} \tag{6}$$

The first term on the right-hand side of Eq. (6) represents the total amount of heat from chilled water; the second-term accounts for the latent heat of vaporization (L) for the amount of refrigerants adsorbed (dq_{ads}/dT) and the sensible heat required to cool down the incoming condensate from the condensation temperature T_{con} to evaporation temperature T_{eva}. The term ε_{eva} in Eq. (6) expresses the heat exchanger effectiveness that came from the log mean temperature difference of the heat exchanger (evaporator) in the flow system. The left-hand side of Eq. (6) represents the sensible heat requirement by the liquid refrigerant and the metal of heat exchanger tubes in the evaporator.

Total Mass Balance

The total mass balance of refrigerant (water) can be expressed as

$$dW_{eva,w} = -W\left(\frac{dq_{des-con}}{dt} + \frac{dq_{ads-eva}}{dt}\right) \tag{7}$$

the where subscripts des-con and ads-eva refer to the vapor flow from desorber to condenser and from evaporator to adsorber.

Adsorption Rate

The combination of the silica-gel adsorption rate was modeled by Sakoda and Suzuki [20] as a function of temperature:

$$dq/dt = k_sa_p.\left(q^* - q\right) \tag{8}$$

The overall mass transfer coefficient, k_sa_p, was estimated by Eqs. (9) and (10):

$$k_sa_p = \frac{15D}{R_p^2} \tag{9}$$

$$D = D_0\exp(-E_a/RT) \tag{10}$$

where D refers to the surface diffusivity. D_o is a constant, and is given as 25.4×10^{-4} m^2/s. E_a expresses the activation energy of surface diffusion, and is given as 4.20×10^4 J/mol. R is the universal gas constant and equals 8.314 J/mol K.

The amount adsorbed in equilibrium, q^*, is predicted by equation as follows:

$$q^* = \frac{0.8\left[P_s\left(T_w\right)/P_s\left(T_s\right)\right]}{1 + 0.5\left[P_s\left(T_w\right)/P_s\left(T_s\right)\right]} \tag{11}$$

where $P_s(T_w)$ and $P_s(T_s)$ are the saturation vapor pressure at temperature T_w (water vapor) and T_s (silica gel), respectively. The saturation vapor pressure and temperature are correlated by Antoine's equation, as follows:

$$P_s = 133.32 \times \exp\left(18.3 - \frac{3820}{T - 46.1}\right) \tag{12}$$

System Performance

Coefficient of performance (COP) and cooling capacity (CC) are mainly characteristics on the performance of the reheat

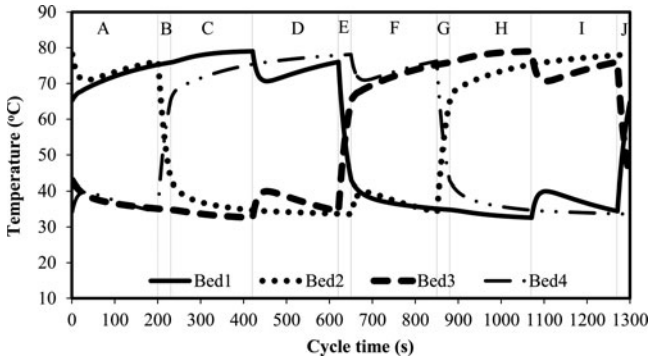

Figure 2 Temperature histories of the four-bed reheat adsorption cycle.

adsorption cycle, can be measured as

$$\mathrm{COP} = \dot{m}_{ch}.C_w \int_0^{t_{cycle}} \left(T_{ch,i} - T_{ch,o}\right) dt \Big/ \times \dot{m}_h.C_w \int_0^{t_{cycle}} \left(T_{h,i} - T_{h,o}\right) dt \quad (13)$$

$$\mathrm{CC} = \dot{m}_{ch}.C_w \int_0^{t_{cycle}} \left(T_{ch,i} - T_{ch,o}\right) {}^{dt}/_{t_{cycle}} \quad (14)$$

OPTIMIZATION METHOD

A cyclic simulation using MATLAB software with ode-45 solver was developed to solve the performance of the reheat cycle based upon the Eqs. (1)–(14), and particle swarm optimization (PSO) is applied to optimized the cycle time components (i.e., adsorption/desorption time, preheating/precooling time, and mass recovery time). In the PSO, cycle time components were chosen as the variable and COP and cooling capacity as the objective functions, respectively. The number of particles, 20, and the number of iterations, 1000, were considered during running the PSO, and it was considered that all of the particles reached their best position before the end of the iterations. The operation mode of the cycle refers to Table 1 during running the simulation. All input parameters and standard operating condition are given in Table 2 and Table 3, respectively.

RESULTS AND DISCUSSION

Temperature Histories

Figure 2 illustrates the temperature histories of the four beds of the chiller with heat-source temperature 60°C and total cycle time 1300 s.

It is worth mentioning here that in the beginning (420 s) bed2 and bed4 are in the mass recovery process where bed2 is in heating mode and bed4 in cooling mode (mode A), respectively.

It was seen that at the beginning, the temperature of bed2 decreased and that of bed4 increased suddenly after that temperature of bed2 was increased and bed4 decreased due to heating by hot water and cooling by cold water, respectively.

As results, bed2 starts to desorb and bed4 starts to adsorb water vapor very rapidly. In mode B, bed2 is in the precooling and bed4 in the preheating process. Thus, the temperature of bed2 decreased and pressure declined. On the other hand, the temperature of bed4 increased. The next process is the adsorption process for bed2 and desorption process for bed4 (modes C, D, and E). In this process, bed2 operates in evaporator pressure and bed4 operates in condenser pressure. Refrigerant in the evaporator will be evaporated and adsorbed by bed2. At the same time, adsorbed refrigerant of bed4 will be released to the condenser in the adsorption process and then condensed in condenser. Up to mode E is a first half-cycle and the next process (mode F to J) is similar to mode A to E; only adsorber and desorber position will be changed for each bed pair, which is obviously observed in this figure.

Water Content in Bed

Figure 3 illustrates the variation of water content in the adsorber/desorber of the bed. Heat-source temperature at 60°C and fixed chilled water outlet temperature at 9°C are applied. Water contents in bed1, bed2, bed3, and bed4 were decreased during the desorption process because vapor is condensed into the condenser (i.e., mode A-B-C for bed1, mode H-I-J for bed2, mode F-G-H for bed3, and mode C-D-E for bed4) and increased during the adsorption process because the bed adsorbed the vapor from the evaporator (i.e., mode F-G-H for bed1, mode C-D-E for bed2, mode A-B-C for bed3, and mode H-I-J for bed4).

During the preheating and precooling process, water contents in all of beds remained constant because all valves on the system were fully closed (i.e., mode E and mode J for bed1 and bed3 and mode B and mode G for bed2 and bed4).

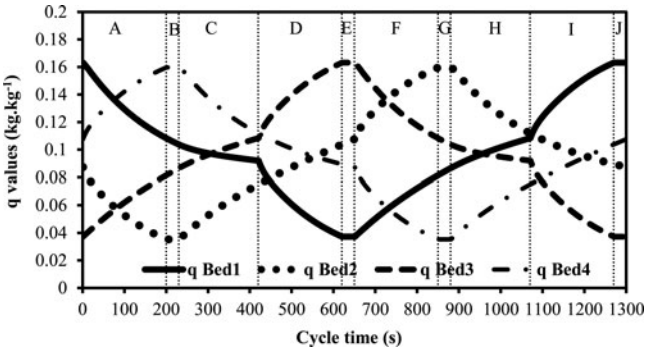

Figure 3 Water content in bed.

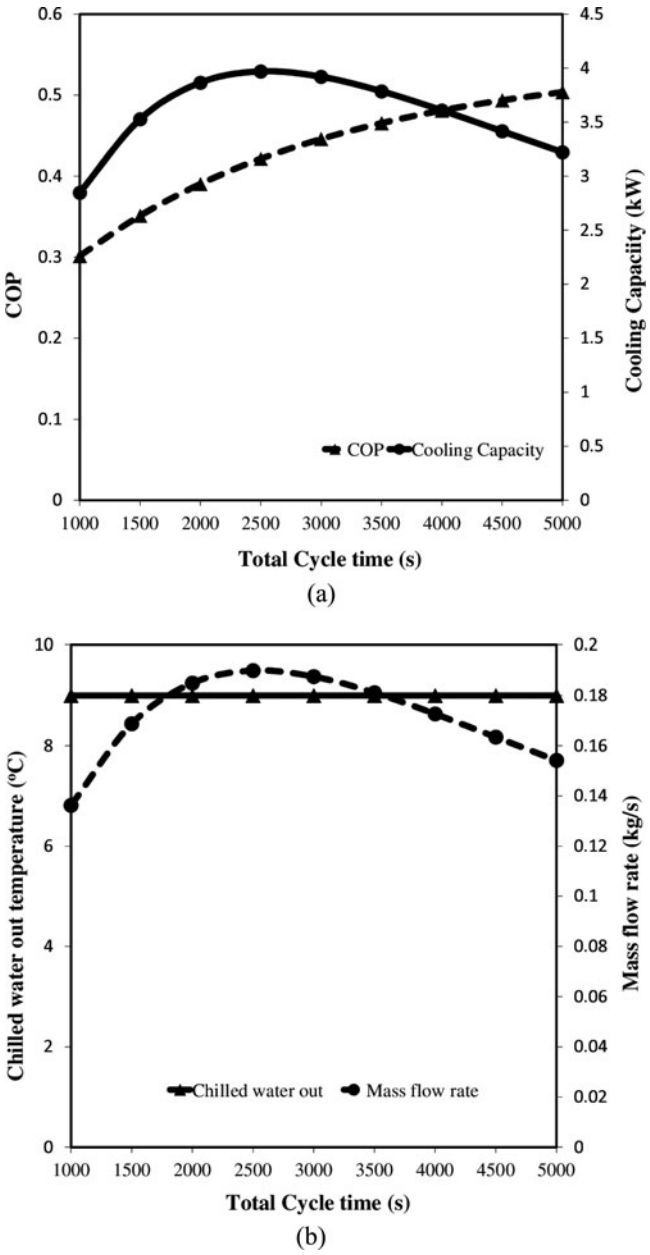

Figure 4 Performance of cycle time.

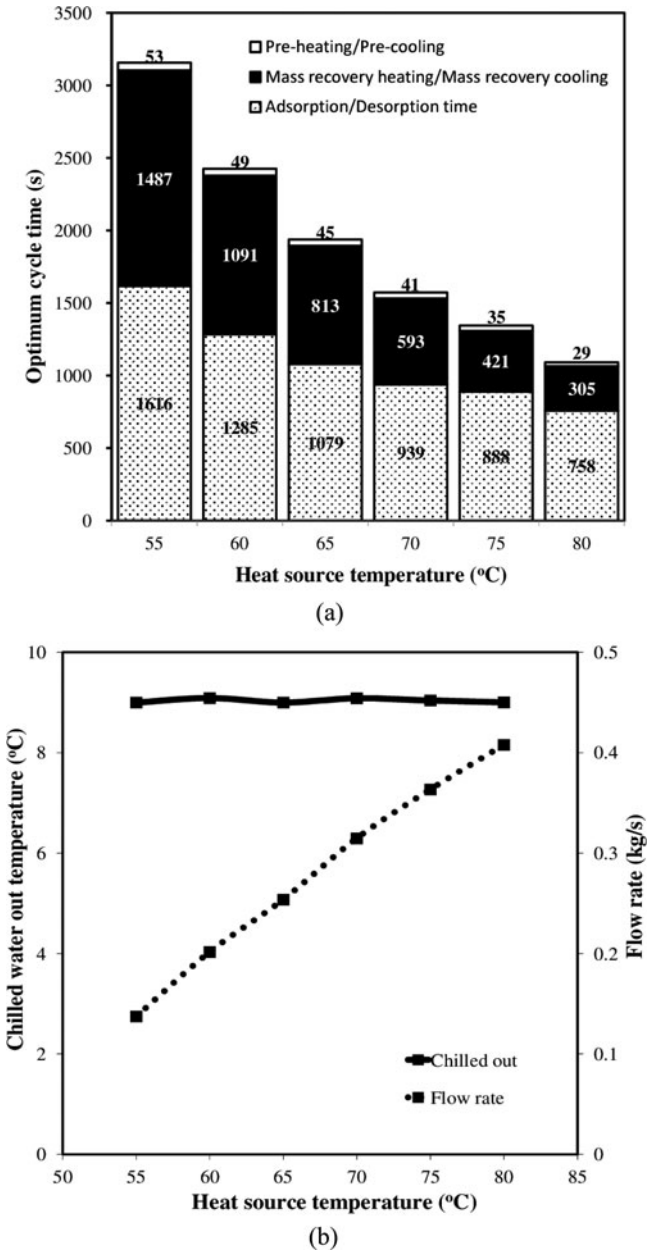

Figure 5 (a) Cycle time optimization and (b) the achievement of chilled water out temperature by controlling mass flow rate.

In the mass recovery with heating process, water content in bed1 was decreased (mode D) because the vapor transferred into bed3; therefore, water content in bed3 increased (mode D), respectively. In the mass recovery with cooling process, water content in bed1 increased (mode I) because of received vapor from bed3, and therefore, water content in bed3 decreased (mode I).

Performance of Cycle Time

The effect of cycle time for the performance and correlation among chilled water out temperature and mass flow rate of the four-bed reheat cycle are presented in Figure 4.

Figure 4a depicts the influences of cycle time on COP and cooling capacity. It was observed that COP increased along with cycle time. Cycle time 1000 s to 5000 s with 500 s escalation applied to show the performance characteristic. Chilled water out temperature applied in fixed condition at 9°C, while controlled mass flow rate was based on Figure 4b. This figure shows that mass flow rate increased due to gain in the chilled water out temperature 9°C in cycle time from 1000 s to 3000 s and decreased when the cycle time was more than 3000 s. The reason is that more refrigerant should be distributed between these ranges to keep chilled water outlet constant. Cycle time from 2000 s to 3000 s required the highest mass flow rate to gain chilled water outlet 9°C.

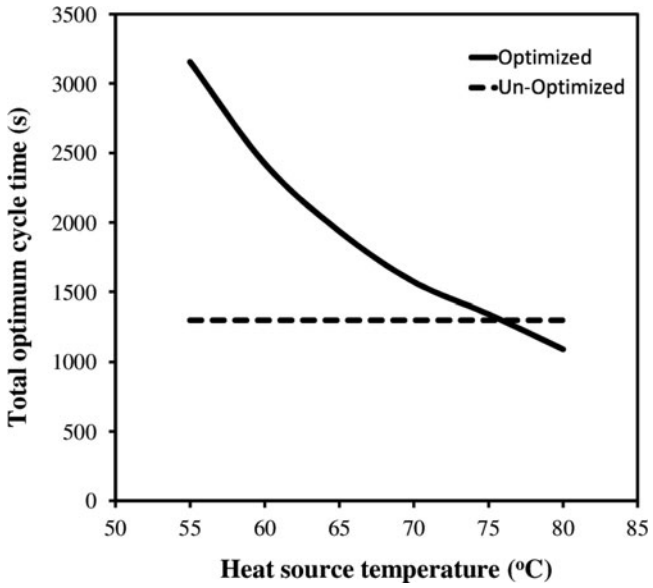

Figure 6 Total optimum cycle time.

The highest cooling capacity values attained at cycle time between 2000 s and 3000 s. Cycle time out of this range made cooling capacity lower. The reason is that the adsorption/desorption process cannot occur well within a long cycle time, and for the short cycle time the process researches its equilibrium state, which causes the cooling capacity to decline smoothly.

Cycle Time Optimization

Cycle time optimization of the four-bed reheat cycle is presented in Figure 5a, and the achievement of chilled water out temperature by controlling mass flow rate is shown in Figure 5b. The cycle optimizations consist of adsorption/desorption time, mass recovery time, and preheating/precooling time. Heat-source temperature from 55 to 80°C was chosen to show its characteristic. For low heat-source temperature (55°C) required longer cycle time to gain the optimum performance. In contrast, the opposite tendency happened with high heat-source temperature (80°C).

From Figure 5b, chilled water flow rate was increased with heat-source temperature to maintain the chilled water outlet temperature at the constant temperatures. To gain chilled water outlet temperature 9°C, mass flow rate should be controlled carefully. Based on Figure 5b, mass flow rate increased along with heat-source temperature. Higher heat-source temperature required more water consumption in evaporator, so the flow rate valve should be opened widely to keep chilled water outlet temperature 9°C.

Figure 6 shows the total cycle time of the reheat cycle after and before optimization. The figure shows that the total cycle time was decreased with the heat-source temperature. For the low heat-source temperature, cycle time optimization increased almost double compared to the cycle with unoptimization. This

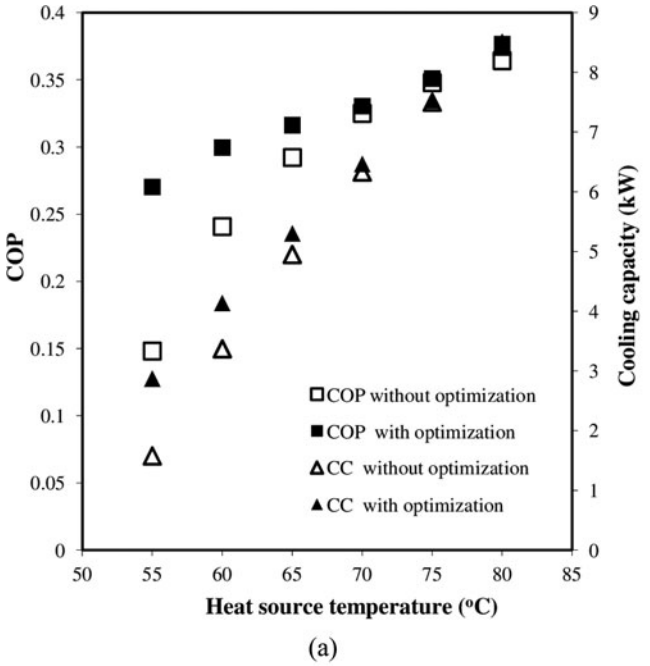

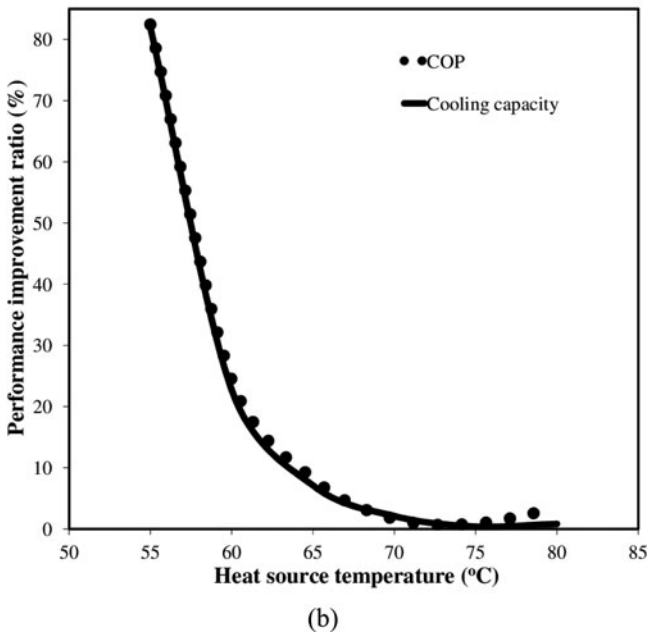

Figure 7 (a) Performance enhancement and (b) performance improvement ratio.

increment influenced by the enhancement in the mass recovery time optimization and decreasing in the preheating/precooling time optimization, respectively.

Performance Enhancement and Comparison

Figure 7a presented the performance enhancement, and Figure 7b refers to the performance improvement ratio of the reheat cycle. For the low heat-source temperature (55–65°C) both COP and cooling capacity of the reheat cycle with

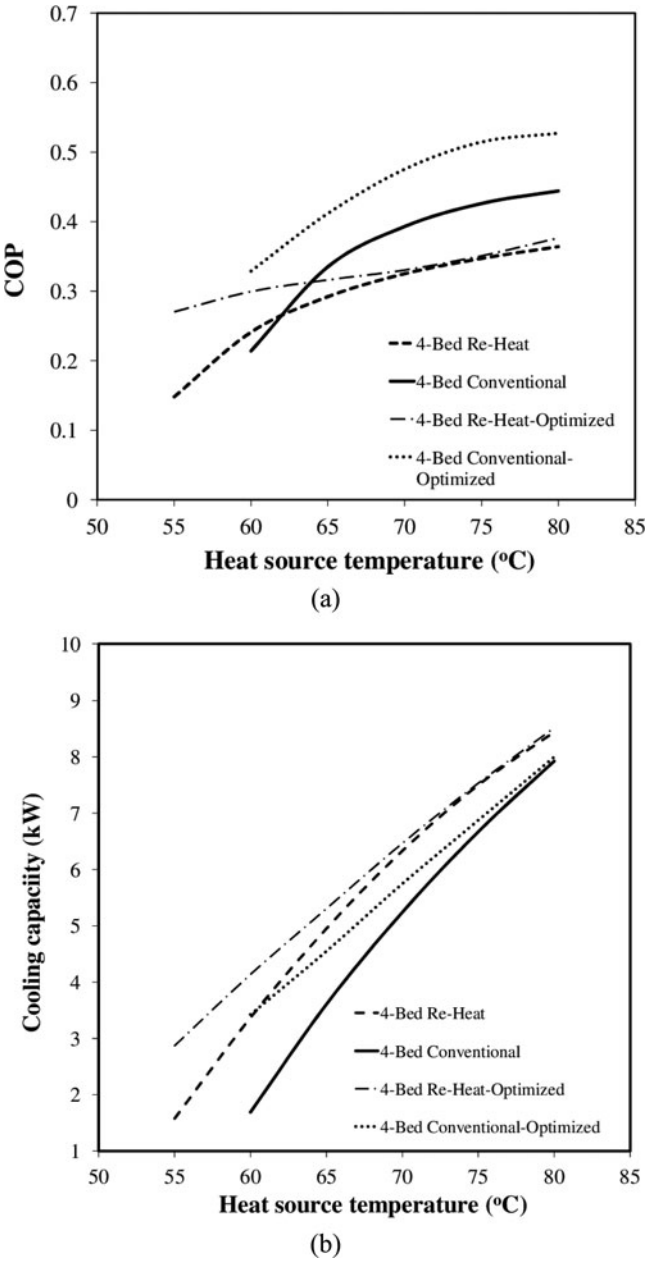

Figure 8 Performance comparison.

optimization rose significantly compared to the high heat-source temperature (70–80°C). The heat-source temperature 55°C showed the highest increment of 80% rise in both COP and cooling capacity, while 20% increment was found for the heat-source temperature 60°C and 7% increment for the heat-source temperature 65°C, respectively. For relatively high heat-source temperature (70-80°C), although there was an increment in both COP and cooling capacity, the value of escalation rose smoothly by about 1%.

From this point of view, cycle time selection based on Table 3, especially for low heat-source temperature before optimization, was not suitable for the best performance achievement and the optimized cycle time based on Figure 5a should be applied. For the high heat-source temperature, although the performance rose slightly, the optimization of cycle time still offered better performance.

Figure 8 presents the optimization performance comparison between the reheat cycle and conventional cycle. The conventional cycle consists of four-adsorber/desorber beds (heat exchangers), one evaporator, and one condenser, such that the upper bed and the lower bed never interact with the evaporator and the condenser. The operation strategy of the conventional cycle goes through only four steps: desorption, precooling, adsorption, and preheating.

From Figure 8, we can observe that the reheat cycle for both COP and cooling capacity offers better performance compared to the conventional cycle, especially for low heat-source temperature. For high heat-source temperature, even the conventional cycle shows a better COP compared with the reheat cycle but the cooling capacity is still lower. On the other hand, the conventional cycle cannot be done with a heat-source temperature of 55°C if operated with the chilled water outlet 9°C. From this point of view, the reheat cycle promises better performance for low heat-source temperature. The optimization of cycle time should be applied in order to enhance the performance of the reheat cycle.

CONCLUSIONS

The optimization of the four-bed reheat cycle was observed during this study while applying a fiexed chilled water out temperature. Controlling the mass flow rate is a necessity in order to gain a fixed chilled water out temperature. Short cycle time (below 3000 s) required a mass flow rate higher than for longer cycle time (up to 3000 s). The COP increased along with cycle time, and the highest cooling capacity values were attained at cycle time between 2000 s and 3000 s.

Cycle optimization of the reheat cycle offered better performance in both COP and cooling capacity. The heat-source temperature 55°C showed the highest increment of 80% rise in both COP and cooling capacity, with a 20% increment for heat-source temperature 60°C and 7% increment for heat-source temperature 65°C, respectively. For relatively high heat-source temperature (70–80°C), although there was an increment in both COP and cooling capacity, the value of escalation raised smoothly by about 1%.

NOMENCLATURE

A	area, m^2
C	specific heat, J/kg-K
CC	cooling capacity, kW
COP	coefficient of performance
D_o	preexponential constant in Eq. (10), m^2/s
Ea	activation energy, J/kg
L	latent heat of vaporization, J/kg

$\dot{m}$	mass flow rate, kg/s
P_s	saturated vapor pressure, Pa
q	concentration, kg refrigerant/kg adsorbent
q^*	concentration at equilibrium, kg refrigerant/kg adsorbent
Q	average heat released, W
Q_s	isosteric heat of adsorption, J/kg
R	gas constant, J/kg
Rp	average radius of a particle, m
T	temperature, K
T_s	saturated vapor temperature, K
t	time, s
U	overall heat transfer coefficient, W/m^2-K
W	weight, kg

Greek Symbols

γ	bed connection indicator
δ	adsorption indicator
ε	heat exchanger efficiency

Subscripts

ads	adsorption
bed	heat exchanger
con	condenser
ch	chilled water
chill	chilled water
cw	cooling water
des	desorption
eva	evaporator
h	hot water
i	inlet
o	outlet
s	sorption element
v	vapor
w	water

REFERENCES

[1] Saha, B. B., Akisawa, A., and Koyama, S., Thermally Powered Sorption Technology, *Japan ISTPST*, pp. 71–74, 2003.

[2] Ng, K. C., Recent Developments in Heat-Driven Silica Gel–Water Adsorption Chiller, *Heat Transfer Engineering*, vol. 24, issue 3, pp. 1–3, 2003.

[3] Dieng, A. O., and Wang, R. Z., Literature Review on Solar Adsorption Technologies for Ice-Making and Air Conditioning Purposes and Recent Developments in Solar Technology, *Renewable and Sustainable Energy Reviews*, vol. 5, pp. 313–342, 2001.

[4] Kashiwagi, T., Akisawa, A., Yoshida, S., Alam, K. C. A., and Hamamoto, Y., Heat Driven Sorption Refrigerating and Air Conditioning Cycle in Japan, *Proceedings of the International Sorption Heat Pump Conference*, Shanghai, China, pp. 50–62, 2002.

[5] Boelman, E., Saha, B. B., and Kashiwagi, T., Experimental Investigation of a Silica Gel-Water Adsorption Refrigeration Cycle—The Influence of Operating Conditions on Cooling Output and COP, *ASHRAE Transactions*, vol. 101, pp. 358–366, 1995.

[6] Saha, B. B., Boelman, E., and Kashiwagi, T., Computer Simulation of a Silica Gel-Water Adsorption Refrigeration Cycle—The Influence of Operating Conditions on Cooling Output and COP, *ASHRAE Transactions*, vol. 101, pp. 348–357, 1995.

[7] Saha, B. B., Akisawa, A., and Kashiwagi, T., Silica Gel–Water Advanced Adsorption Refrigeration Cycle, *Energy*, vol. 22, pp. 437–444, 1997.

[8] Karagiorgas, M, and Meunier, F., The Dynamics of a Solid-Adsorption Heat Pump Connected With Outside Heat Sources of Finite Capacity, *Heat Recovery Systems and CHP*, vol. 7, pp. 285–299, 1987.

[9] Critoph, R. E., and Zhong, Y., Review of Trends in Solid Sorption Refrigeration and Heat Pumping Technology, *Proc. IMechE, Part E: Journal of Process Mechanical Engineering*, vol. 219, pp. 285–300, 2005.

[10] Saha, B. B., Koyama, S., Lee, J. B., Kuwahara, K., Alam, K. C. A., Hamamoto, Y., Akisawa, A., and Kashiwagi, T., Performance Evaluation of a Low-Temperature Waste Heat Driven Multi-Bed Adsorption Chiller, *International Journal of Multiphase Flow*, vol. 29, pp. 1249–1263, 2003.

[11] Saha, B. B., El-Sharkawi, I. I., Koyama, S., Lee, J. B., and Kuwahara, K., Waste Heat Driven Multi-Bed Adsorption Chiller: Heat Exchanger Overall Thermal Conductance on Chiller Performance, *Heat Transfer Engineering*, vol. 27, issue 5, pp. 80–87, 2007.

[12] Ahmed, R. M. R., and Raya, K. A., Physical and Operating Conditions Effects on Silica Gel/Water Adsorption Chiller Performance, *Applied Energy*, vol. 89, pp. 142–149, 2012.

[13] Rahman, A. F. M. M., Miyazaki, T., Ueda, Y., Saha, B. B., and Akisawa, A., Performance Comparison of Three-Bed Adsorption Cooling System With Optimal Cycle Time, *Heat Transfer Engineering*, vol. 34, issue 11–12, pp. 938–947, 2013.

[14] Alam, K. C. A., Kang, Y. T., Saha, B. B., Akisawa, A., and Kashiwagi, T., A Novel Approach to Determine Optimum Switching Frequency of a Conventional Adsorption Chiller, *Energy*, vol. 28, pp. 1021–1037, 2003.

[15] Alam, K. C. A., Khan, M. Z. I., Uyun, A. S., Hamamoto, Y., Akisawa, A., and Kashiwagi, T., Experimental Study of a Low Temperature-Heat Driven Re-Heat Two-Stage Adsorption Chiller, *Applied Thermal Engineering*, vol. 27, pp. 1686–1692, 2007.

[16] Uyun, A. S., Akisawa, A., Miyazaki, T., Ueda, Y., and Kashiwagi, T., Numerical Analysis of an Advanced

Three-Bed Mass Recovery Adsorption Refrigeration Cycle, *Applied Thermal Engineering*, vol. 29, pp. 2876–2884, 2009.

[17] Khan, M. Z. I., Alam, K. C. A., Saha, B. B., Akisawa, A., and Kashiwagi, T., Study on a Re-Heat Two-Stage Adsorption Chiller—The Influence of Thermal Capacitance Ratio, Overall Thermal Conductance Ratio and Adsorbent Mass on System Performance, *Applied Thermal Engineering*, vol. 27, pp. 1677–1685, 2007.

[18] Chua, H. T., Kim Choon, N. G., Malek, A., Kahiwagi, T., Akisawa, A., and Saha, B. B., A Regenerative Adsorption Process and Multi-Reactor Regenerative Adsorption Chiller, World Intellectual Application Published Under the Patent Cooperation Treaty (PCT), June 15, 2000.

[19] Wirajati, I. G. A. B., Akisawa, A., Ueda, Y., and Miyazaki, T., Experimental Investigation of a Reheating Two-Stage Adsorption Chiller Applying Fixed Chilled Water Outlet Conditions, *Heat Transfer Research*, HTR-6774, doi:10.1615/HeatTransRes.2014007186, 2014.

[20] Sakoda, A., and Suzuki, M., Fundamental Study on Solar Powered Adsorption Cooling System, *Journal Chemical Engineering of Japan*, vol. 17, pp. 52–57, 1984.

I Gusti Agung Bagus Wirajati obtained his bachelor's degree from Udayana University, Bali, Indonesia, in 1996 and completed his M.Eng. in Tokyo University of Agriculture and Technology in 2007, respectively. He has been working at the Bali State Polytechnic since 1999, and is now on study leave and doing his Ph.D. research on thermally driven adsorption chillers at Tokyo University of Agriculture and Technology, Tokyo, Japan. He has published four articles in peer-reviewed journals and international conference proceedings.

Yuki Ueda obtained his bachelor's and master's degrees from Nagoya University, Japan, in 2000 and 2002, respectively. He received his Ph.D. in engineering from the same university in 2005. He has been an associate professor at Tokyo University of Agriculture and Technology, Japan, since 2006. His research interests are thermally driven systems including adsorption chillers/heat pumps and thermoacoustic engines and refrigerators.

Atsushi Akisawa obtained bachelors and master's degrees from Tokyo University, Japan, in 1985 and 1987, respectively. He received his Ph.D. in engineering from the same university in 1997. He joined Tokyo University of Agriculture and Technology as a lecturer in 1997 and has been a professor since 2007. His research field covers thermally driven heat pumps, solar thermal utilization, energy system analysis, and technological evaluation of energy saving. He is a fellow of the Japan Society of Mechanical Engineers and a board member of the Japan Solar Energy Society.

Takahiko Miyazaki obtained his bachelor's degree from Chuo University, Japan, in 1995 and his M.Sc. in renewable energy and architecture from University of Nothingham, United Kingdom, in 2003. He received his Ph.D. in engineering from the Tokyo University of Agriculture and Technology, Japan, in 2005. He was an assistant professor at Tokyo University of Agriculture and Technology from 2005 to 2010. Since 2011, he has been an associate professor in the Faculty of Engineering Sciences, Kyushu University, Japan. His main research interests are thermally driven air-conditioning systems including adsorption chillers/heat pumps and desiccant air conditioning.